Axion window on new macroscopic forces

Luca Di Luzio,[1,*] Hector Gisbert,[2,1,3,†] Fabrizio Nesti,[4,5,‡] and Philip Sørensen[2,1,§]

[1] *Istituto Nazionale di Fisica Nucleare, Sezione di Padova, Via Francesco Marzolo 8, 35131 Padova, Italy*
[2] *Dipartimento di Fisica e Astronomia "G. Galilei", Università di Padova, Via Francesco Marzolo 8, 35131 Padova, Italy*
[3] *Escuela de Ciencias, Ingeniería y Diseño, Universidad Europea de Valencia, Passeig de la Petxina 2, 46008 Valencia, Spain*
[4] *Dipartimento di Scienze Fisiche e Chimiche, Università dell'Aquila, Via Vetoio, I-67100, L'Aquila, Italy*
[5] *Istituto Nazionale di Fisica Nucleare, Laboratori Nazionali del Gran Sasso, I-67100 Assergi (AQ), Italy*

(Received 31 July 2024; accepted 4 December 2024; published 24 December 2024)

Axion-mediated forces are enhanced by the presence of *CP*-violating axion couplings, which are however tightly constrained by electric dipole moment (EDM) searches. We discuss the underlying hypotheses behind different sources of *CP* violation at high energies and the interplay between axion-mediated force experiments and EDM observables. Specifically, we identify various mechanisms, based on new sources of *CP* violation or Peccei-Quinn symmetry breaking, that can significantly relax EDM constraints, leading to a substantial redefinition of the QCD axion window for axion-mediated forces. By considerably enlarging the QCD axion parameter space, our results provide a well-motivated target for experiments probing scalar axion couplings to matter fields. These include fifth-force tests of gravity, as well as searches for spin-dependent forces via precision magnetometry, proton storage rings and ultracold molecules.

DOI: 10.1103/PhysRevD.110.115034

I. INTRODUCTION

The quantum chromodynamics (QCD) axion originally emerged from the need to "wash out" *CP* violation from strong interactions [1–4]. This is achieved by introducing the axion field a, endowed with a Peccei-Quinn (PQ) shift symmetry that renders the QCD topological angle θ unphysical. Hence, the issue of *CP* violation in strong interactions is traded for a dynamical question about the axion vacuum expectation value (VEV), yielding an effective θ parameter

$$\theta_{\text{eff}} \equiv \frac{\langle a \rangle}{f_a}, \tag{1}$$

where f_a is the axion decay constant and the electric dipole moment (EDM) of the neutron (nEDM) demands $|\theta_{\text{eff}}| \lesssim 10^{-10}$ [5].

A general result [6] ensures that the QCD ground state energy density is minimal for $\theta_{\text{eff}} = 0$. However, one relies on the fact that QCD is a vector-like theory and does not have extra sources of *CP* violation beyond the θ term. Both conditions are violated in the Standard Model (SM), which is a chiral theory that features a *CP*-violating (CPV) phase in the quark sector. Indeed, in Ref. [7] it was estimated $\theta_{\text{eff}}^{\text{SM}} \sim 10^{-19}$ (see also [8–10]). While this irreducible SM contribution to θ_{eff} turns out to be too tiny to be testable, new CPV sources beyond the SM, generically expected to explain the baryon asymmetry of the universe, might lead to a value of θ_{eff} closer to the nEDM bound.

An axion VEV could also be generated from ultraviolet (UV) sources of PQ symmetry breaking. This is motivated by the fact that the $\mathrm{U}(1)_{\text{PQ}}$, as a global symmetry, does not need to be exact and it is expected to be broken at least by quantum gravity effects (see e.g. [11]).

Whatever its origin, a striking consequence of $\theta_{\text{eff}} \neq 0$ is the generation of a *scalar* axion coupling to nucleons, $g^S_{aN}(\theta_{\text{eff}}, \ldots) \propto \theta_{\text{eff}}$ [12], where the ellipses stand for other sources of *CP* violation, to be discussed in this work. Including both scalar (g^S_{af}) and pseudo-scalar (g^P_{af}) couplings to matter fields, with $f = p, n, e$ [cf. Eq. (2)], one obtains different types of nonrelativistic potentials mediated by the light axion field, leading to new macroscopic forces, as suggested long ago by Moody and Wilczek [12]. Remarkably, scalar axion couplings, being

*Contact author: luca.diluzio@pd.infn.it
†Contact author: hector.gisbert@pd.infn.it
‡Contact author: fabrizio.nesti@aquila.infn.it
§Contact author: philip.soerensen@pd.infn.it

spin-independent, strongly enhance axion-mediated forces compared to the case of pseudo-scalar couplings. An updated review of axion-mediated force experiments and relevant limits can be found in Ref. [13] (see also [14–16]).

While phenomenological analyses often focus on a naive definition of the QCD axion band, based on the simplifying assumption that $\theta_{\rm eff}$ is the only source of CP violation [12], more recent studies have started to systematically analyze different sources of CP violation and their nontrivial interplay with EDM searches [17–23].

In this work, we provide a fresh look at the UV origin of the g^S_{af} coupling and identify different mechanisms, based on new sources of CP or PQ breaking, in order to maximize the scalar axion coupling relative to EDM constraints, thus leading to a substantial redefinition of the traditional QCD axion window for axion-mediated forces.

II. AXION COUPLINGS TO MATTER

Including both CP-conserving and CPV couplings, the axion effective Lagrangian with matter fields ($f = p, n, e$) reads

$$\mathcal{L}_{af} = -g^P_{af} a \bar{f} i\gamma_5 f - g^S_{af} a \bar{f} f, \tag{2}$$

where $g^P_{af} = C_{af} m_f / f_a$ and the dimensionless couplings C_{af} are model-dependent $\mathcal{O}(1)$ numbers. As a benchmark scenario, we consider here the DFSZ model [24,25] at large $\tan\beta$, yielding $C_{ap} = 0.6$, $C_{an} = -0.3$ and $C_{ae} = 1/3$ (see e.g. [26] for a derivation). The QCD axion mass and decay constant follow the standard relation $m_a \simeq 5.7(10^9\ {\rm GeV}/f_a)$ eV.

In the traditional QCD axion scenario with a nonzero $\theta_{\rm eff}$, for g^S_{aN} ($N = p, n$) one can use the standard isospin-symmetric formula of Moody and Wilczek [12], with the correct extra $1/2$ factor [18], which gives at most

$$g^{S,\theta}_{aN} \simeq 2 \times 10^{-21} \left(\frac{10^9\ {\rm GeV}}{f_a} \right), \tag{3}$$

assuming maximal $\theta_{\rm eff} = 1.2 \times 10^{-10}$, saturating the d_n constraint. The value (3) defines the upper side of the traditional QCD axion band for axion-mediated forces, currently employed for instance in [27]. The lower side of the band is estimated through the irreducible SM contribution, via the CKM phase, as [19]

$$g^{S,{\rm CKM}}_{aN} \simeq 10^{-30} \left(\frac{10^9\ {\rm GeV}}{f_a} \right). \tag{4}$$

Note, however, that a CPV scalar coupling to nucleons g^S_{aN} can arise from various mechanisms related to new sources of CP or PQ violation. These can lead to (a) new terms in the meson plus axion chiral Lagrangian (χPT), that induce a shift of the axion and chiral vacuum leading to CPV couplings [28], but also to (b) direct CPV axion-nucleon terms in the baryon chiral Lagrangian (BχPT).

Experimental searches typically operate at the atomic level rather than directly probing g^S_{af}. When considering an atomic system ${}^A_Z X$, the axion scalar coupling is effectively described by the average

$$g^S_{aX} \equiv \frac{A - Z}{A} g^S_{an} + \frac{Z}{A} g^S_{ap} + \frac{Z}{A} g^S_{ae}. \tag{5}$$

In our theoretical predictions, we will consider the case of Tungsten ($A = 184, Z = 74$) which pertains to ARIADNE [29,30]. Other elements, relevant for fifth-force searches, imply a relative variation from the Tungsten benchmark that is below the 10% level.

In the following, we explore the possibility of maximizing this scalar axion-matter coupling in comparison to $g^{S,\theta}_{aX}$, equal to the traditional $g^{S,\theta}_{aN}$ in the isospin limit, while satisfying the EDM constraints.

III. CPV COUPLINGS FROM χPT

In the χPT Lagrangian, the terms generated by CP or PQ breaking lead to a realignment of the vacuum, namely a nonzero $\theta_{\rm eff}$ together with π_0, η_8 and η_0 meson VEVs if chiral symmetry is also broken. These four vacuum shifts induce CPV baryon couplings in the BχPT Lagrangian, reported for completeness in the Appendix. It is important to note that the induced couplings generally depend on just *three* combinations. Indeed, the BχPT Lagrangian feels the vacuum realignment only via the three quark masses, the only spurions of chiral $SU(3)_V \times U(3)_A$. As a result, all effects depend on the following three chiral phases (with $q = u, d, s$)

$$\alpha_q = \left[\frac{\lambda_3}{2} \frac{\langle \pi_0 \rangle}{F_\pi} + \frac{\lambda_8}{2} \frac{\langle \eta_8 \rangle}{F_\pi} + \frac{\mathbf{1}}{\sqrt{6}} \frac{\langle \eta_0 \rangle}{F_\pi} \right]_{qq} + \frac{m_* \theta_{\rm eff}}{2 m_q}, \tag{6}$$

where the λ's are the Gell-Mann matrices, $m_* = (m_u^{-1} + m_d^{-1} + m_s^{-1})^{-1}$, and the pion decay constant is $F_\pi \simeq 92$ MeV. For the neutron and proton CPV couplings, one can rewrite the results of [18] (see also [31,32]) in a simple and general way in terms of α's

$$\begin{aligned} g^S_{ap,n} &= -\frac{8 m_* B_0}{f_a} \left(b_0 \sum_q \alpha_q + b_+ \alpha_{u,d} + b_- \alpha_s \right) \\ &\simeq 10^{-11} \frac{10^9\ {\rm GeV}}{f_a} (2.4 \alpha_{u,d} + 2.8 \alpha_{d,u} + 1.5 \alpha_s), \end{aligned} \tag{7}$$

with 20% hadronic uncertainties, see Appendix for details. Expressions in terms of α's can be derived also for nucleon-meson CPV couplings (cf. Appendix) so that this fact holds in general even for EDM observables. We thus find that from χPT there is a model-independent correlation between EDMs and $g^S_{ap,n}$, all driven by three phases $\alpha_{u,d,s}$.

IV. EDM CONSTRAINTS ON CPV COUPLINGS

We focus first on the CPV effects induced in χPT, considering the $g^S_{an,p}$ terms in Eq. (5), with g^S_{ae} set to zero. The strongest EDM limits are currently imposed by neutron and Mercury. For them, we find the constraints

$$\frac{d_n}{d_n^<} \simeq 10^{10}|3.7\alpha_u + 5.9\alpha_d + 40.0\alpha_s| \lesssim 1, \quad (8)$$

$$\frac{d_{\rm Hg}}{d_{\rm Hg}^<} \simeq 10^{10}|3.1\alpha_u + 5.0\alpha_d + 36.0\alpha_s| \lesssim 1, \quad (9)$$

with 10% and 50% hadronic uncertainties respectively, see Appendix for details. Here, $d_n^< = 1.8 \times 10^{-26}$ e cm [5] and $d_{\rm Hg}^< = 6.3 \times 10^{-30}$ e cm [33] are the experimental bounds on the neutron and Mercury EDM, respectively.

While other nuclei lead to weaker bounds, more constraints arise from EDMs of paramagnetic systems from the contribution of two-photon exchange processes between electrons and the nucleus induced by CP-odd semileptonic interactions [34]. The most stringent one, set by paramagnetic ThO [35], leads to the additional constraint (cf. Appendix)

$$10^{10}|0.11\alpha_u - 0.22\alpha_d| \lesssim 1, \quad (10)$$

with 10% hadronic uncertainties, see Appendix for details. The limit in Eq. (10) is slightly weaker, but together with Eqs. (8) and (9), constrain all α's to be of the order of $10^{-9\div10}$. This implies that the axion scalar coupling in Eq. (7) cannot deviate much from the traditional value. Including uncertainties, we find at most $|g^S_{aX}/g^{S,\theta}_{aX}| \lesssim \mathcal{O}(10)$.

In conclusion, the three EDM constraints fix the three phases, impeding a relevant enhancement of g^S_{aX} relative to the traditional QCD axion case $g^{S,\theta}_{aX}$. This result is model-independent, as far as χPT-induced effects are concerned.

The situation could potentially change with direct contributions to the BχPT Lagrangian. New terms in general lead to additional combinations different from those in Eq. (6), possibly evading the EDM limits. The possible new operators, classified in [20], suffer from uncertainties in the low-energy constants (LECs), not determined by chiral symmetry, and a model-independent analysis is premature. One can, of course, imagine that more operators conspire to bypass the EDM constraints while allowing for a larger g^S_{aX}. This scenario, hard to obtain in predictive theories, could be checked in specific models.

To this aim, theoretical work on the LECs would be most welcome, while on the experimental side future improvements on EDMs such as Radon [36] will also be important to sharpen the connection between EDMs and g^S_{aN}.

V. SEMILEPTONIC OPERATORS

We turn here to CPV effects induced only by the scalar axion-electron coupling g^S_{ae}, the third term in Eq. (5). This coupling can be generated by semileptonic operators as

$$\mathcal{L}_{\rm sl} = C^P_{\rm eq}(\bar{e}_L e_R)(\bar{q}\gamma_5 q) + \text{H.c.}, \quad (11)$$

with implicit sum over $q = u,\ d,\ s$. After the canonical axion-dependent chiral rotation of the quarks (cf. Appendix), Eq. (11) leads to [20]

$$g^S_{ae} = \frac{m_* B_0 F_\pi^2}{2f_a} \text{Im} \sum_q \frac{1}{m_q} C^P_{\rm eq}. \quad (12)$$

The interactions in Eq. (11) also generate 4-fermion operators involving nucleons and electrons [20]

$$\mathcal{L}_{eN} = -\frac{G_F}{\sqrt{2}} \Big\{ i\bar{e}\gamma_5 e \bar{N}(C_S^{(0)} + \tau_3 C_S^{(1)})N + \bar{e}e \frac{\partial_\mu}{m_N} [\bar{N}(C_P^{(0)} + \tau_3 C_P^{(1)}) S^\mu N] \Big\}, \quad (13)$$

where $N = (pn)^T$ is the nucleon doublet, S^μ is its spin, G_F is the Fermi constant, and $C^{(0,1)}_{S,P}$ are the Wilson coefficients encoding the short-distance coefficients C^P_{eq} of Eq. (11). The Mercury EDM or CPV effects induced in polar molecules like ThO [35], YbF [37], and HfF [38] receive contributions from $C^{(0,1)}_{S,P}$. Using Eq. (25) in Ref. [20], we find the conditions on the $C^P_{\rm eq}$ to cancel them

$$C^P_{eu} = C^P_{ed} = C^P_{es} \equiv C, \quad (14)$$

for some C. These conditions still allow for a nonzero g^S_{ae} from Eq. (12)

$$g^S_{ae} = -\frac{B_0 F_\pi^2}{2f_a} \text{Im} C. \quad (15)$$

Hence, strikingly, the EDM limits are evaded for flavor universal semileptonic couplings. The coefficient ImC is constrained by the high-p_T tails of the $pp \to \ell\ell$ Drell-Yan processes. The results in Ref. [39] imply Im$C \lesssim (2\ \text{TeV})^{-2}$, which allows for a substantial enhancement of the scalar axion coupling, $|g^S_{aX}/g^{S,\theta}_{aX}| \lesssim 1 \times 10^3$.

VI. PQ-BREAKING AS THE ORIGIN OF CPV COUPLINGS

Another possibility to generate a scalar axion coupling to fermions is to consider a source of PQ breaking, which also breaks CP in the axion sector. A common choice is provided by operators of the type $\mathcal{L}_{\rm \not{PQ}} \supset -e^{i\delta}\phi^n \Lambda^{-n+4}$, with δ a generic phase, Λ is the UV scale at which the operator is generated, and $\phi = \frac{f_a}{\sqrt{2}} e^{ia/f_a}$ is a complex scalar where the axion is the angular mode and the radial mode is integrated out. Including the QCD axion potential, $V_{\rm QCD} = -\chi_{\rm QCD} \cos\frac{a}{f_a}$ with $\chi_{\rm QCD} \approx (76~{\rm MeV})^4$, the induced axion VEV reads $\theta_{\rm eff} \simeq -2^{1-\frac{n}{2}} n \Lambda^{4-n} f_a^n \sin\delta/\chi_{\rm QCD}$. Note that such a PQ-breaking scenario directly matches to the traditional QCD axion coupling in Eq. (3).

Another class of operators, recently discussed in Refs. [40–42], takes the generic form $(\phi/\Lambda)^n \mathcal{O}_{\rm SM}$, where $\mathcal{O}_{\rm SM}$ is an operator made of SM fields. To maximize the contribution to g_{aX}^S in Eq. (5), relative to EDM bounds, we consider a ϕ^n coupling to the electron Yukawa,[1]

$$\mathcal{L}_{\not{\rm PQ}} \supset -e^{i\delta}\left(\frac{\phi}{\Lambda}\right)^n \frac{\sqrt{2}m_e}{v} \bar{L}_L H e_R + {\rm H.c.}, \qquad (16)$$

where $v = 246$ GeV. This operator generates a scalar axion-electron coupling directly at tree level

$$g_{ae}^S = n\left(\frac{f_a}{\sqrt{2}\Lambda}\right)^n \frac{m_e}{f_a}\sin\delta, \qquad (17)$$

and, after setting $\langle H\rangle = (0 v/\sqrt{2})^T$, it also leads to an axion tadpole, $V_{\not{\rm PQ}} = -\sigma a + \ldots$, at one loop. In the leading-log approximation, we find

$$\sigma(\mu) = \frac{n}{2\pi^2}\left(\frac{f_a}{\sqrt{2}\Lambda}\right)^n \frac{m_e^4}{f_a}\sin\delta \ln\left(\frac{v}{\mu}\right), \qquad (18)$$

where μ denotes the renormalization scale. Including the contribution of the QCD axion potential, we obtain the induced axion VEV

$$\theta_{\rm eff} \simeq \frac{n}{2\pi^2}\left(\frac{f_a}{\sqrt{2}\Lambda}\right)^n \frac{m_e^4}{\chi_{\rm QCD}}\sin\delta \ln\left(\frac{v}{1~{\rm GeV}}\right), \qquad (19)$$

where we took $\mu = 1$ GeV to assess the nEDM bound. By using Eq. (19) to express Eq. (17) in terms of $\theta_{\rm eff}$, we obtain

$$g_{ae}^S = \frac{2\pi^2}{\ln(\frac{v}{1~{\rm GeV}})}\frac{\chi_{\rm QCD}}{m_e^3 f_a}\theta_{\rm eff}. \qquad (20)$$

The nEDM bound, $|\theta_{\rm eff}| \lesssim 10^{-10}$, provides the main limiting factor for this coupling,[2] which in this scenario dominates by far the atomic average in Eq. (5), allowing for $|g_{aX}^S/g_{aX}^{S,\theta}| \lesssim 2\times 10^7$.

[1]Similar operators with ϕ^n coupled to light quarks or gluons yield an unsuppressed long-distance contribution to $\theta_{\rm eff}$ [40], preventing a significant contribution to g_{aX}^S.

[2]Other direct contributions to EDMs come from axion exchange involving $aG\tilde{G}$ and $a\bar{e}e$ vertices, leading to semileptonic operators as in Eq. (13). Using results from [43], we obtain $g_{ae}^S \lesssim 2.2(f_a/10^9~{\rm GeV})$ from ThO EDM, which is negligible compared to the bound from nEDM in Eq. (20).

VII. $Z_{\mathcal{N}}$ AXION

The last possibility that we consider is a modification of the standard m_a–f_a QCD relation, suppressing m_a for fixed f_a. This can be achieved by employing $\mathcal{N}$ mirror copies of the SM [44–46], with $\mathcal{N}$ odd and ${\rm SM}_k \to {\rm SM}_{k+1({\rm mod}\,\mathcal{N})}$ under the $Z_{\mathcal{N}}$ symmetry and the axion acting nonlinearly: $a \to a + 2\pi k/\mathcal{N}$, with $k = 0, \ldots, \mathcal{N}-1$. In this way, the axion potential gets exponentially suppressed and, in the large $\mathcal{N}$ limit, the axion mass relative to the standard QCD axion mass scales as [45]

$$\frac{(m_a)_{\mathcal{N}}^2}{m_a^2} \simeq \frac{\sqrt{1-z^2}(1+z)}{\sqrt{\pi}}\mathcal{N}^{3/2} z^{\mathcal{N}-1}, \qquad (21)$$

where $z = m_u/m_d \simeq 0.48$. In these scenarios, an important constraint on f_a arises from the fact that the exponential axion mass suppression is spoiled by finite density effects in stellar environments [47]. In particular, the strongest constraints arise from the modifications of the mass-radius relationship of white dwarfs, which exclude $33 \le \mathcal{N} \le 69$ [48]. Assuming $\mathcal{N} \le 31$, we find $|g_{aX}^S/g_{aX}^{S,\theta}| \lesssim 5\times 10^3$.

VIII. AXION-MEDIATED FORCE EXPERIMENTS

Depending on the combination of couplings involved, axion-mediated nonrelativistic potentials can be of three types: $g_{af}^S g_{af}^S$ (monopole-monopole), $g_{af}^S g_{af}^P$ (monopole-dipole), or $g_{af}^P g_{af}^P$ (dipole-dipole). The idea of searching for dipole-dipole axion interactions in atomic physics is as old as the axion itself [3]. However, dipole-dipole forces turn out to be spin-suppressed and suffer from large backgrounds from ordinary magnetic forces. Furthermore, our models enhance only scalar couplings and thus do not improve the situation for dipole-dipole interactions. Hence, in the following, we will focus on monopole-monopole and monopole-dipole interactions, whose parameter space is displayed in Fig. 1.

In this figure, the conventional QCD axion region is represented by an orange band, whose upper (lower) side is set by the scalar coupling in Eq. (3) [Eq. (4)], while for the pseudo-scalar couplings we employed the predictions of the DFSZ model at large $\tan\beta$ [cf. discussion below Eq. (2)]. Among the models discussed in this work, we consider three examples, given respectively by the inclusion of CPV semileptonic operators (red), the $Z_{\mathcal{N}}$ axion model with modified m_a–f_a relation (purple), and the PQ-breaking electron Yukawa scenario (blue). These extend the conventionally expected range of scalar couplings. The figure should be understood so that the bands overlap from below, such that, e.g., the PQ-breaking model predicts a coupling between the upper limit of the blue band and down to the lower limit of the minimal QCD axion band (orange). See previous sections for how the upper limits on the scalar coupling is obtained in nonminimal QCD axion models.

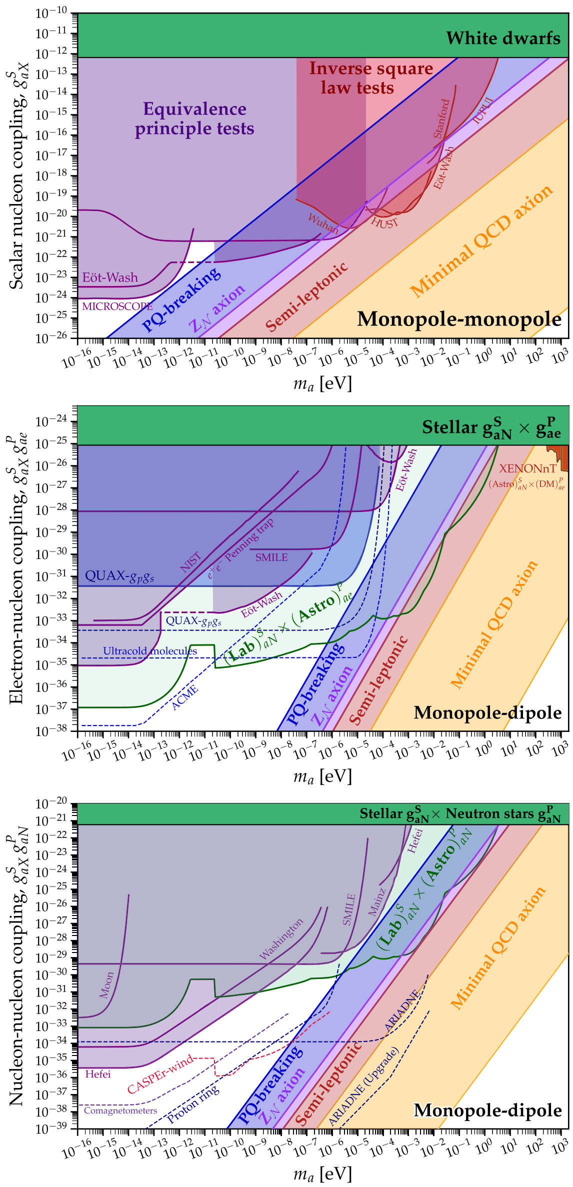

FIG. 1. QCD axion window for axion-mediated forces vs current constraints (full lines) and future experimental sensitivities (dashed lines). Here g^S_{aX} is the effective scalar axion-atom coupling defined in Eq. (5). Figure adapted from [13,27].

The top panel of Fig. 1 displays searches based on monopole-monopole interactions. In contrast with gravity, these long-range forces deviate from the inverse-square law and depend on the material's composition. Tests of the inverse-square law [49–55] can reach parameter space from all three models presented here. At longer ranges, i.e., lower axion masses, composition dependence becomes more important than deviations from the inverse-square law. This enables searches for violations of the equivalence principle [56,57] to probe the parameter space offered by the $Z_{\mathcal{N}}$ and the PQ-breaking models.

These results suggest that improvements in tests of the equivalence principle or the inverse square law have the chance to discover these particular types of QCD axions.

Another interesting opportunity is given by monopole-dipole searches, whose limits (full lines) and projected sensitivities (dashed lines) are reported in the middle and lower panels of Fig. 1 for the case of pseudoscalar axion couplings to electrons (g^P_{ae}) and nucleons (g^P_{aN}), respectively. In particular, ARIADNE [29,30] aims to probe the monopole-dipole force generated by a rotating source mass and detected via nucleon spins, employing precision magnetometry. A similar approach is pursued by QUAX-$g_p g_s$ [58–60], using instead electron spins. Several other experiments have established bounds or are attempting to improve the sensitivity to either $g^S_{aX} g^P_{ae}$ [61–71] or $g^S_{aX} g^P_{aN}$ [70–73] couplings. Regardless of which pseudoscalar coupling is employed, our scenarios considerably improve the prospects for monopole-dipole searches. The projected reaches of QUAX-$g_p g_s$ as well as proposals based on ultracold molecules [69] and proton storage rings [73] can probe parameter space beyond the traditional QCD band which is populated by the models studied here, while ARIADNE would be able to test wide ranges of parameter space, also inside the minimal QCD axion band.

IX. CONCLUSIONS

In this paper, we have reconsidered the UV origin of the g^S_{af} coupling and identified various mechanisms based on new sources of *CP* or PQ breaking. These mechanisms can significantly relax EDM constraints, leading to a substantial redefinition of the traditional QCD axion window for axion-mediated forces, as shown in Fig. 1. Our findings suggest an expanded QCD axion parameter space, providing strong motivation for pushing the current limits on the search for new macroscopic forces.

ACKNOWLEDGMENTS

We thank Antonio Rodríguez-Sánchez and Alessio Maiezza for useful discussions. The work of L. D. L., H. G., and P. S. is supported by the European Union—NextGeneration EU and by the University of Padua under the 2021 STARS Grants@Unipd programme (Acronym and title of the project: CPV-Axion—Discovering the *CP*-violating axion) as well as by the European Union—Next Generation EU and by the Italian Ministry of University and Research (MUR) via the PRIN 2022 project n. 2022K4B58X—AxionOrigins.

APPENDIX: BARYON-MESON COUPLINGS CONTRIBUTIONS TO EDMS

In this Appendix, we discuss the contributions of baryon-meson couplings to the neutron and proton

EDMs. The leading order (LO) baryon chiral Lagrangian can be written as

$$\begin{aligned}\mathcal{L}_{\mathrm{B}} = {}& \mathrm{Tr}[\bar{B} i\gamma^\mu(\partial_\mu B + [\Gamma_\mu, B]) - M_B \bar{B}B] \\ & - \frac{D}{2}\mathrm{tr}[\bar{B}\gamma^\mu\gamma_5\{\xi_\mu, B\}] - \frac{F}{2}\mathrm{tr}[\bar{B}\gamma^\mu\gamma_5[\xi_\mu, B]] \\ & - \frac{\lambda}{2}\mathrm{tr}[\xi_\mu]\mathrm{tr}[\bar{B}\gamma^\mu\gamma_5 B] + b_D \mathrm{tr}[\bar{B}\{\chi_+, B\}] \\ & + b_F \mathrm{tr}[\bar{B}[\chi_+, B]] + b_0 \mathrm{tr}[\chi_+]\mathrm{tr}[\bar{B}B], \end{aligned} \tag{A1}$$

where we employed the definitions

$$B = \begin{pmatrix} \frac{1}{\sqrt{2}}\Sigma^0 + \frac{1}{\sqrt{6}}\Lambda^0 & \Sigma^+ & p \\ \Sigma^- & -\frac{1}{\sqrt{2}}\Sigma^0 + \frac{1}{\sqrt{6}}\Lambda^0 & n \\ \Xi^- & \Xi^0 & -\frac{2}{\sqrt{6}}\Lambda^0 \end{pmatrix},$$
$$U = \xi_R \xi_L^\dagger \qquad (\xi_R = \xi_L^\dagger), \tag{A2}$$

and $\Gamma_\mu \equiv \frac{1}{2}\xi_R^\dagger(\partial_\mu - ir_\mu)\xi_R + \frac{1}{2}\xi_L^\dagger(\partial_\mu - il_\mu)\xi_L$, $\xi_\mu \equiv i\xi_R^\dagger(\partial_\mu - ir_\mu)\xi_R - i\xi_L^\dagger(\partial_\mu - il_\mu)\xi_L$, $\chi_+ \equiv \xi_L^\dagger \chi \xi_R + \xi_R^\dagger \chi^\dagger \xi_L$.

Here, M_B denotes the baryon mass in the chiral limit, while $\chi = 2B_0 \mathrm{diag}\{m_u, m_d, m_s\}$ is the chiral spurion including the quark masses. In Eq. (A1), the interaction terms proportional to D, F and λ are CP conserving, while those proportional to b_D, b_F and b_0 violate CP. The D and F LECs are extracted from baryon semileptonic decays, and they read at tree level $D \simeq 0.8$ and $F \simeq 0.5$ [74]. The LEC B_0 is given by $B_0 = m_\pi^2/(m_d + m_u)$, while $b_{D,F}$ are determined from the baryon octet mass splittings, $b_D \simeq 0.07\ \mathrm{GeV}^{-1}$, $b_F \simeq -0.21\ \mathrm{GeV}^{-1}$ at LO [28]. The value of b_0 is determined from the pion-nucleon sigma-term as $b_0 \simeq -\sigma_{\pi N}/4m_\pi^2$. From [75,76] one obtains $b_0 = -0.76 \pm 0.04\ \mathrm{GeV}^{-1}$ at 90% confidence level. The LEC λ is unknown and is set to zero. We also defined the shorthand $b_\pm = b_D \pm b_F$.

The QCD θ-term plus the axion is rotated away by an appropriate axion-dependent chiral rotation of the quark fields, $q_L \to e^{-i\alpha_q} q_L$, $q_R \to e^{i\alpha_q} q_R$, with $\alpha_q = (\theta + \frac{a}{f_a}) m_*/2m_q$ [28]. By applying this diagonal $U(3)_A$ field transformation on the $\xi_{L,R}$ and the baryon chiral fields, the axion is effectively included in the meson Lagrangian as well as in the baryon Lagrangian (A1). With this choice of α_q the axion does not mix with π^0 and η_8.

In the presence of new physics in the χPT Lagrangian, one has to further rotate the U fields to have $\langle U \rangle = 1$, as well as to shift the axion field. This again amounts to a diagonal rotation (we consider strangeness preserving interactions here) so that one can consider altogether three generic α_q, incorporating the mesons and axion VEVs, as in Eq. (6) in the main text. As already mentioned, this *global* chiral rotation is effectively equivalent to a rotation of the spurions of chiral $SU(3)_V \times U(3)_A$, namely a rotation of the quark masses in the meson and baryon chiral Lagrangian (A1), as follows: $m_q \to m_q e^{2i\alpha_q}$.

It is this phase rotation that generates, from the baryon Lagrangian, the various CPV baryon interactions with the physical meson fields [28,77]. We parametrize their couplings as $\mathcal{L}_{\mathrm{B}\chi\mathrm{PT}}^{\mathrm{CPV}} \supset \bar{g}_{ABC} ABC$, where A, B are baryon fields and C is a meson, and their expressions are reported below.

The neutron and proton EDMs are generated at loop level and can be expressed, following e.g. Ref. [78], in terms of these couplings and loop functions, which are expanded at leading order in the meson masses. We write $d_{n,p} = \sum_i d_{n,p}^{(i)}$, where the index i runs over all baryon-meson couplings contributing to the neutron and proton EDMs. Specifically, for the neutron EDM, only two couplings contribute [78]

$$d_n^{(\bar{n}p\pi^-)} = \frac{e(F+D)\bar{g}_{\bar{n}p\pi^-}(\pi m_\pi - 2m_N \log(m_\pi^2/m_N^2))}{16\sqrt{2}F_\pi m_N \pi^2}, \tag{A3}$$

$$d_n^{(\bar{n}\Sigma^- K^+)} = \frac{e(F-D)\bar{g}_{\bar{n}\Sigma^- K^+}(\pi m_K - 2m_N \log(m_K^2/m_N^2))}{16\sqrt{2}F_\pi m_N \pi^2}, \tag{A4}$$

while more couplings contribute to the proton EDM due to its electric charge

$$\begin{aligned} d_p^{(\bar{p}p\pi^0)} &= -\frac{e(D+F)\bar{g}_{\bar{p}p\pi^0} m_\pi}{16\sqrt{2}F_\pi m_N \pi}, \\ d_p^{(\Sigma^+\bar{p}K^0)} &= -\frac{e(D-F)\bar{g}_{\Sigma^+\bar{p}K^0} m_K}{8\sqrt{2}F_\pi m_N \pi}, \end{aligned} \tag{A5}$$

$$\begin{aligned} d_p^{(\bar{p}p\eta_8)} &= -\frac{e(D-3F)\bar{g}_{\bar{p}p\eta_8} m_{\eta_8}}{48\sqrt{2}F_\pi m_N \pi}, \\ d_p^{(\bar{p}p\eta_0)} &= -\frac{e(2D+3\lambda)\bar{g}_{\bar{p}p\eta_0} m_{\eta_0}}{24\sqrt{2}F_\pi m_N \pi}, \end{aligned} \tag{A6}$$

$$d_p^{(n\bar{p}\pi^+)} = -\frac{e(D+F)\bar{g}_{n\bar{p}\pi^+}(3\pi m_\pi - 2m_N \log(m_\pi^2/m_N^2))}{16\sqrt{2}F_\pi m_N \pi^2}, \tag{A7}$$

$$d_p^{(\bar{p}\Lambda^0 K^+)} = -\frac{e(D+3F)\bar{g}_{\bar{p}\Lambda^0 K^+}(3\pi m_K - 2m_N \log(m_K^2/m_N^2))}{96\sqrt{2}F_\pi m_N \pi^2}, \tag{A8}$$

$$d_p^{(\Sigma^0\bar{p}K^+)} = -\frac{e(D-F)\bar{g}_{\Sigma^0\bar{p}K^+}(3\pi m_K - 2m_N \log(m_K^2/m_N^2))}{32\sqrt{2}F_\pi m_N \pi^2}. \tag{A9}$$

For the couplings in terms of phases, we find

$$\bar{g}_{\bar{n}p\pi^-} = -\frac{4\sqrt{2}B_0 b_+(m_d\alpha_d + m_u\alpha_u)}{F_\pi}, \qquad \bar{g}_{\bar{n}\Sigma^- K^+} = -\frac{4\sqrt{2}B_0 b_-(m_u\alpha_u + m_s\alpha_s)}{F_\pi}, \tag{A10}$$

and

$$\bar{g}_{n\bar{p}\pi^+} = -\frac{4\sqrt{2}B_0 b_+(m_d\alpha_d + m_u\alpha_u)}{F_\pi}, \qquad \bar{g}_{\Sigma^+\bar{p}K^0} = -\frac{4\sqrt{2}B_0 b_-(m_d\alpha_d + m_s\alpha_s)}{F_\pi}, \tag{A11}$$

$$\bar{g}_{\bar{p}\Lambda^0 K^+} = -\frac{4B_0(b_D + 3b_F)(m_s\alpha_s + m_u\alpha_u)}{\sqrt{3}F_\pi}, \qquad \bar{g}_{\Sigma^0\bar{p}K^+} = -\frac{4\sqrt{2}B_0 b_-(m_s\alpha_s + m_u\alpha_u)}{F_\pi}, \tag{A12}$$

$$\bar{g}_{\bar{p}p\pi^0} = \frac{8B_0[b_0(m_d\alpha_d - m_u\alpha_u) - b_+ m_u\alpha_u]}{F_\pi}, \qquad \bar{g}_{nn\pi^0} = \frac{8B_0[b_0(m_d\alpha_d - m_u\alpha_u) + b_+ m_d\alpha_d]}{F_\pi}, \tag{A13}$$

$$\bar{g}_{\bar{p}p\eta_8} = \frac{8B_0[b_0(2m_s\alpha_s - m_u\alpha_u - m_d\alpha_d) + 2(b_D - b_F)m_s\alpha_s - (b_D + b_F)m_u\alpha_u]}{\sqrt{3}F_\pi}, \tag{A14}$$

$$\bar{g}_{\bar{p}p\eta_0} = -\frac{8\sqrt{\frac{2}{3}}B_0[b_0(m_u\alpha_u + m_d\alpha_d + m_s\alpha_s) + (b_D - b_F)m_s\alpha_s + (b_D + b_F)m_u\alpha_u]}{\sqrt{3}F_\pi}. \tag{A15}$$

In the above formulas, we have taken the large N_C-limit $F_\pi \simeq F_0$, with F_π and F_0 being the pion and the eta decay constants, respectively.

Taking these results into account, we obtain the relevant EDMs in terms of generic phases

$$d_p = \{\alpha_u(-1.72^{+0.19}_{-0.24}) \times 10^{-15} + \alpha_d(-2.63^{+0.14}_{-0.16}) \times 10^{-15} + \alpha_s(-1.31^{+0.25}_{-0.30}) \times 10^{-14}\} e\,\mathrm{cm}, \tag{A16}$$

$$d_n = \{\alpha_u(6.7^{+0.7}_{-0.9}) \times 10^{-16} + \alpha_d(10.6^{+0.6}_{-0.7}) \times 10^{-16} + \alpha_s(7.1^{+0.5}_{-0.5}) \times 10^{-15}\} e\,\mathrm{cm}, \tag{A17}$$

where hadronic uncertainties from LECs and quark masses have been included. By considering the impact of the neutron and proton EDMs on the Mercury EDM [20], we find

$$d_{\mathrm{Hg}} = \{\alpha_u(-2.0^{+0.6}_{-0.7}) \times 10^{-19} + \alpha_d(-3.1^{+1.1}_{-1.2}) \times 10^{-19} + \alpha_s(-23 \pm 11) \times 10^{-19}\} e\,\mathrm{cm}. \tag{A18}$$

The neutron and Mercury EDM expressions should be compared with the experimental bounds, respectively $d_n^< = 1.8 \times 10^{-26}$ e cm [5] and $d_{\mathrm{Hg}}^< = 6.3 \times 10^{-30}$ e cm [33].

The ThO EDM bound finally amounts to $\bar{g}^{(1)}_{\pi NN} \lesssim 4 \times 10^{-10}$ [34], with

$$\begin{aligned}\bar{g}^{(1)}_{\pi NN} &\equiv \frac{1}{2}(\bar{g}_{nn\pi} + \bar{g}_{pp\pi}) \\ &= \frac{4B_0(2b_0 + b_D + b_F)(\alpha_d m_d - \alpha_u m_u)}{F_\pi} \\ &= (0.42^{+0.05}_{-0.07})\alpha_u + (-0.89^{+0.04}_{-0.05})\alpha_d.\end{aligned} \tag{A19}$$

Eqs. (A17)–(A19) translate into the constraints of Eqs. (9) and (10) in the main text.

We finally look for $\alpha_{u,d,s}$ that, while respecting these constraints, try to maximize the CPV coupling in Eq. (5), which numerically is

$$\begin{aligned}g^S_{aX} = {}& 10^{-11}\frac{10^9\,\mathrm{GeV}}{f_a} \\ &\times [(2.6^{+0.4}_{-0.5})\alpha_u + (2.6^{+0.4}_{-0.5})\alpha_d + (1.50^{+0.21}_{-0.27})\alpha_s].\end{aligned} \tag{A20}$$

We find that all $\alpha_{u,d,s}$ are constrained to be of order $O(10^{-9\div 10})$, and lead to a maximal value of

$$\left|\frac{g^S_{aX}}{g^{S,\theta}_{aX}}\right| \lesssim 10, \tag{A21}$$

allowing also for the uncertainties in Eqs. (A17)–(A19).

[1] R. D. Peccei and H. R. Quinn, Phys. Rev. Lett. **38**, 1440 (1977).
[2] R. D. Peccei and H. R. Quinn, Phys. Rev. D **16**, 1791 (1977).
[3] S. Weinberg, Phys. Rev. Lett. **40**, 223 (1978).
[4] F. Wilczek, Phys. Rev. Lett. **40**, 279 (1978).
[5] C. Abel *et al.*, Phys. Rev. Lett. **124**, 081803 (2020).
[6] C. Vafa and E. Witten, Phys. Rev. Lett. **53**, 535 (1984).
[7] H. Georgi and L. Randall, Nucl. Phys. **B276**, 241 (1986).
[8] J. R. Ellis and M. K. Gaillard, Nucl. Phys. **B150**, 141 (1979).
[9] I. B. Khriplovich, Phys. Lett. B **173**, 193 (1986).
[10] J.-M. Gérard and P. Mertens, Phys. Lett. B **716**, 316 (2012).
[11] R. Kallosh, A. D. Linde, D. A. Linde, and L. Susskind, Phys. Rev. D **52**, 912 (1995).
[12] J. E. Moody and F. Wilczek, Phys. Rev. D **30**, 130 (1984).
[13] C. A. J. O'Hare and E. Vitagliano, Phys. Rev. D **102**, 115026 (2020).
[14] G. Raffelt, Phys. Rev. D **86**, 015001 (2012).
[15] I. G. Irastorza and J. Redondo, Prog. Part. Nucl. Phys. **102**, 89 (2018).
[16] P. Sikivie, Rev. Mod. Phys. **93**, 015004 (2021).
[17] M. Pospelov, Phys. Rev. D **58**, 097703 (1998).
[18] S. Bertolini, L. Di Luzio, and F. Nesti, Phys. Rev. Lett. **126**, 081801 (2021).
[19] S. Okawa, M. Pospelov, and A. Ritz, Phys. Rev. D **105**, 075003 (2022).
[20] W. Dekens, J. de Vries, and S. Shain, J. High Energy Phys. 07 (2022) 014.
[21] V. Plakkot, W. Dekens, J. de Vries, and S. Shain, J. High Energy Phys. 11 (2023) 012.
[22] L. Di Luzio, G. Levati, and P. Paradisi, J. High Energy Phys. 02 (2024) 020,
[23] L. Di Luzio, H. Gisbert, G. Levati, P. Paradisi, and P. Sørensen, arXiv:2312.17310.
[24] A. R. Zhitnitsky, Sov. J. Nucl. Phys. **31**, 260 (1980).
[25] M. Dine, W. Fischler, and M. Srednicki, Phys. Lett. **104B**, 199 (1981).
[26] L. Di Luzio, M. Giannotti, E. Nardi, and L. Visinelli, Phys. Rep. **870**, 1 (2020).
[27] C. O'Hare, cajohare/axionlimits: Axionlimits, https://cajohare.github.io/AxionLimits/ (2020).
[28] A. Pich and E. de Rafael, Nucl. Phys. **B367**, 313 (1991).
[29] A. Arvanitaki and A. A. Geraci, Phys. Rev. Lett. **113**, 161801 (2014).
[30] A. A. Geraci *et al.* (ARIADNE Collaboration), Springer Proc. Phys. **211**, 151 (2018).
[31] V. Cirigliano, W. Dekens, J. de Vries, and E. Mereghetti, Phys. Lett. B **767**, 1 (2017).
[32] S. Bertolini, A. Maiezza, and F. Nesti, Phys. Rev. D **101**, 035036 (2020).
[33] B. Graner, Y. Chen, E. G. Lindahl, and B. R. Heckel, Phys. Rev. Lett. **116**, 161601 (2016); **119**, 119901(E) (2017).
[34] V. V. Flambaum, M. Pospelov, A. Ritz, and Y. V. Stadnik, Phys. Rev. D **102**, 035001 (2020).
[35] V. Andreev *et al.* (ACME Collaboration), Nature (London) **562**, 355 (2018).
[36] M. Bishof *et al.*, Phys. Rev. C **94**, 025501 (2016).
[37] J. J. Hudson, D. M. Kara, I. J. Smallman, B. E. Sauer, M. R. Tarbutt, and E. A. Hinds, Nature (London) **473**, 493 (2011).
[38] W. B. Cairncross, D. N. Gresh, M. Grau, K. C. Cossel, T. S. Roussy, Y. Ni, Y. Zhou, J. Ye, and E. A. Cornell, Phys. Rev. Lett. **119**, 153001 (2017).
[39] L. Allwicher, D. A. Faroughy, F. Jaffredo, O. Sumensari, and F. Wilsch, J. High Energy Phys. 03 (2023) 064.
[40] Y. Zhang, Phys. Rev. D **107**, 055025 (2023).
[41] Y. Zhang, Phys. Rev. Lett. **132**, 081003 (2024).
[42] L. Di Luzio and P. Sørensen, J. High Energy Phys. 10 (2024) 239.
[43] L. Di Luzio, R. Gröber, and P. Paradisi, Phys. Rev. D **104**, 095027 (2021).
[44] A. Hook, Phys. Rev. Lett. **120**, 261802 (2018).
[45] L. Di Luzio, B. Gavela, P. Quilez, and A. Ringwald, J. High Energy Phys. 05 (2021) 184.
[46] L. Di Luzio, B. Gavela, P. Quilez, and A. Ringwald, J. Cosmol. Astropart. Phys. 10 (**2021**) 001.
[47] A. Hook and J. Huang, J. High Energy Phys. 06 (2018) 036.
[48] R. Balkin, J. Serra, K. Springmann, S. Stelzl, and A. Weiler, Phys. Rev. D **109**, 095032 (2024).
[49] Y. J. Chen, W. K. Tham, D. E. Krause, D. Lopez, E. Fischbach, and R. S. Decca, Phys. Rev. Lett. **116**, 221102 (2016).
[50] D. J. Kapner, T. S. Cook, E. G. Adelberger, J. H. Gundlach, B. R. Heckel, C. D. Hoyle, and H. E. Swanson, Phys. Rev. Lett. **98**, 021101 (2007).
[51] J. G. Lee, E. G. Adelberger, T. S. Cook, S. M. Fleischer, and B. R. Heckel, Phys. Rev. Lett. **124**, 101101 (2020).
[52] A. A. Geraci, S. J. Smullin, D. M. Weld, J. Chiaverini, and A. Kapitulnik, Phys. Rev. D **78**, 022002 (2008).
[53] S.-Q. Yang, B.-F. Zhan, Q.-L. Wang, C.-G. Shao, L.-C. Tu, W.-H. Tan, and J. Luo, Phys. Rev. Lett. **108**, 081101 (2012).
[54] W.-H. Tan *et al.*, Phys. Rev. Lett. **124**, 051301 (2020).
[55] J. Ke, J. Luo, C.-G. Shao, Y.-J. Tan, W.-H. Tan, and S.-Q. Yang, Phys. Rev. Lett. **126**, 211101 (2021).
[56] G. L. Smith, C. D. Hoyle, J. H. Gundlach, E. G. Adelberger, B. R. Heckel, and H. E. Swanson, Phys. Rev. D **61**, 022001 (2000).
[57] J. Bergé, P. Brax, G. Métris, M. Pernot-Borràs, P. Touboul, and J.-P. Uzan, Phys. Rev. Lett. **120**, 141101 (2018).
[58] N. Crescini, C. Braggio, G. Carugno, P. Falferi, A. Ortolan, and G. Ruoso, Nucl. Instrum. Methods Phys. Res., Sect. A **842**, 109 (2017).
[59] N. Crescini, C. Braggio, G. Carugno, P. Falferi, A. Ortolan, and G. Ruoso, Phys. Lett. B **773**, 677 (2017).
[60] N. Crescini, G. Carugno, P. Falferi, A. Ortolan, G. Ruoso, and C. C. Speake, Phys. Rev. D **105**, 022007 (2022).
[61] D. J. Wineland, J. J. Bollinger, D. J. Heinzen, W. M. Itano, and M. G. Raizen, Phys. Rev. Lett. **67**, 1735 (1991).
[62] B. R. Heckel, E. G. Adelberger, C. E. Cramer, T. S. Cook, S. Schlamminger, and U. Schmidt, Phys. Rev. D **78**, 092006 (2008).
[63] S. A. Hoedl, F. Fleischer, E. G. Adelberger, and B. R. Heckel, Phys. Rev. Lett. **106**, 041801 (2011).
[64] W. A. Terrano, E. G. Adelberger, J. G. Lee, and B. R. Heckel, Phys. Rev. Lett. **115**, 201801 (2015).
[65] Y. V. Stadnik, V. A. Dzuba, and V. V. Flambaum, Phys. Rev. Lett. **120**, 013202 (2018).
[66] J. Lee, A. Almasi, and M. Romalis, Phys. Rev. Lett. **120**, 161801 (2018).

[67] V. A. Dzuba, V. V. Flambaum, I. B. Samsonov, and Y. V. Stadnik, Phys. Rev. D **98**, 035048 (2018).
[68] X. Fan and M. Reig, arXiv:2310.18797.
[69] P. Agrawal, N. R. Hutzler, D. E. Kaplan, S. Rajendran, and M. Reig, J. High Energy Phys. 07 (2024) 133.
[70] C. Baruch, P. B. Changala, Y. Shagam, and Y. Soreq, Phys. Rev. Lett. **133**, 113202 (2024).
[71] C. Baruch, P. B. Changala, Y. Shagam, and Y. Soreq, Phys. Rev. Res. **6**, 043115 (2024).
[72] K. Wei, T. Zhao, X. Fang, Z. Xu, C. Liu, Q. Cao, A. Wickenbrock, Y. Hu, W. Ji, and D. Budker, Phys. Rev. Lett. **130**, 063201 (2023).
[73] P. Agrawal, D. E. Kaplan, O. Kim, S. Rajendran, and M. Reig, Phys. Rev. D **108**, 015017 (2023).
[74] S. Scherer and M. R. Schindler, *A Primer for Chiral Perturbation Theory* (Springer, Berlin, Heidelberg, 2012), Vol. 830.
[75] M. Hoferichter, J. Ruiz de Elvira, B. Kubis, and U.-G. Meißner, Phys. Rev. Lett. **115**, 092301 (2015).
[76] M. Hoferichter, J. Ruiz de Elvira, B. Kubis, and U.-G. Meißner, Phys. Lett. B **760**, 74 (2016).
[77] H. An, X. Ji, and F. Xu, J. High Energy Phys. 02 (2010) 043.
[78] F.-K. Guo and U.-G. Meissner, J. High Energy Phys. 12 (2012) 097.